Estimating Interception from Near-Surface Soil Moisture Response

Subodh Acharya[1*], Daniel McLaughlin[2], David Kaplan[3], and Matthew J. Cohen[1]

1 – School of Forest Resources and Conservation, University of Florida, Gainesville FL
2 – Department of Forest Resources and Conservation, Virginia Tech, Blacksburg, VA
3 – Environmental Engineering Sciences Department, University of Florida, Gainesville FL

* – Corresponding Author

Abstract

Interception is the storage and subsequent evaporation of rainfall by above-ground structures, including canopy and groundcover vegetation and surface litter. Accurately quantifying interception is critical for understanding how ecosystems partition incoming precipitation, but it is difficult and costly to measure, leading most studies to rely on modeled interception estimates. Moreover, forest interception estimates typically focus only on canopy storage, despite the potential for substantial interception by groundcover vegetation and surface litter. In this study, we developed an approach to quantify "total" interception losses (i.e., including forest canopy, understory, and surface litter layers) using measurements of shallow soil moisture dynamics during rainfall events. Across 36 pine and mixed forest stands in Florida (USA), we used soil moisture and rainfall data to estimate the interception storage capacity (β_s), a parameter required to estimate total annual interception losses (I_a) relative to rainfall (R). Estimated values for β_s (mean β_s = 0.30 cm; $0.01 \leq \beta_s \leq 0.62$ cm) and I_a/R (mean I_a/R = 0.14; $0.06 \leq I_a/R \leq 0.21$) were consistent with reported literature values for these ecosystems and were significantly predicted by forest structural attributes (leaf area index and percent groundcover), as well as other site variables (e.g., water table depth). The best-fit model was dominated by LAI and explained nearly 80% of observed β_s variation. These results suggest that whole-forest interception can be measured using a single near-surface soil moisture time series and highlight the variability in interception losses across a single forest type, underscoring the need for expanded empirical measurement. Potential cost savings and logistical advantages of this method relative to conventional, labor-intensive interception measurements may improve empirical estimation of this critical water budget element.

Deleted: such as

Deleted: water use

Deleted: forcing

Deleted: models.

Deleted: capacity for

Deleted: to also intercept rainfall.

Deleted: empirically estimate

Deleted: from the

Deleted: groundcover

Deleted: measured

Deleted: determined

Deleted: which was then used

Deleted:). Calculated

Deleted: both

Deleted: within the ranges

Deleted: in

Deleted: well

Deleted:)

Deleted: well as soil moisture conditions, suggesting total interception (i.e., storage across canopy, groundcover, and litter)

Deleted: . Moreover,

Deleted: considerable spatial variation observed with standard interception measurements, which necessitates intensive sampling, was reduced using this approach, with

Deleted: coefficient of variation among within-plot estimates of 18%. Indeed, less than a quarter of the total variance was at the within-stand level. The proposed method offers several cost

Deleted: , and thus

Deleted: Page Break

Introduction

Rainfall interception (I) is the fraction of incident rainfall stored by above-ground ecosystem structures (i.e., vegetation and litter layers) and subsequently returned to the atmosphere via evaporation (E), never reaching the soil surface and thus never directly supporting transpiration (T) [*Savenije*, 2004]. Interception depends on climate and vegetation characteristics and can be as high as 50% of gross rainfall [*Gerrits et al.,* 2007; 2010; *Calder*, 1990]. Despite being critical for accurate water budget enumeration [*David et al.*, 2005], interception is often disregarded or lumped with evapotranspiration (ET) in hydrological models [*Savenije*, 2004]. Recent work suggests interception uncertainty constrains efforts to partition ET into T and E, impairing representation of water use and yield in terrestrial ecosystems [*Wei et al.,* 2017].

When interception is explicitly considered, it is typically empirically estimated or modeled solely for the tree canopy. For example, direct measurements are often obtained from differences between total rainfall and water that passes through the canopy to elevated above-ground collectors (throughfall) plus water that runs down tree trunks (stemflow) during natural [e.g., *Bryant et al.,* 2005, *Ghimire et al.,* 2012, 2016] or simulated [e.g., *Guevara-Escobar et al.,* 2007; *Putuhena and Cordery,* 1996] rainfall events. This method yields the rainfall fraction held and subsequently lost by the canopy but ignores interception by understory vegetation and litter. Alternatively, numerous empirical [e.g., *Merriam,* 1960], process-based [e.g., *Rutter et al.,* 1971, 1975; *Gash,* 1979, 1995, *Liu*, 1998], and stochastic [*Calder,* 1986] models are available for estimating interception. As with direct measurements, most model applications consider only canopy storage despite groundcover (both understory vegetation and litter layers) interception that can exceed canopy values [*Gerrits and Savenije*, 2011; *Putuhena and Cordery,* 1996]. As

Deleted: nor

Deleted:

Deleted: ic

Deleted: landscape

Deleted: ,

Deleted: other water balance components (e.g.,

Deleted: ,

Deleted: I

Deleted: om

Deleted: However, similar to

Deleted: focus on

Deleted: . Groundcover

Deleted: reservoirs can, in some cases, be higher than canopy such, it seems likely that conventional measures and typical model applications underestimate actual (i.e., “total”) interception.

New field approaches are needed to improve quantification of total interception and refine the calibration and application of available models. A detailed review of available interception models [*Muzylo et al.*, 2009] stresses the need for direct interception measurements across forest types and hydroclimatic regions, but meeting this need will require substantial methodological advances. Throughfall measurements yield direct and site-specific interception estimates [e.g., *Ghimire et al.*, 2017; *Bryant et al.*, 2005], but they are difficult and costly to implement even at the stand scale because of high spatial and temporal variability in vegetation structure. Moreover, comprehensive measurements also require enumeration of spatially heterogeneous stemflow, as well as interception storage by the understory and litter layers, greatly exacerbating sampling complexity and cost [*Lundberg et al.*,1997]. Empirical techniques that estimate total interception, integrate across local spatial and temporal variation, and minimize field installation complexity are clearly desirable.

Here we present a novel approach for estimating total (i.e., canopy, understory and litter) interception using continuously logged, near-surface soil moisture. Prior to runoff generation, infiltration is equivalent to rainfall minus total interception, and the response of near-surface soil moisture during and directly following rain events can be used to inform interception parameters and thus interception losses. Since soil moisture is relatively easy and economical to measure continuously for extended periods, successful inference of interception from soil moisture time series may greatly expand the temporal and spatial domains of empirical interception measurements. As a proof-of-concept, we tested this simple interception estimation method in 36

Deleted:], indicating

Deleted: almost certainly

Deleted: , thereby,

Deleted: o

Deleted: [*Muzylo et al.*, 2009]. Meeting

Deleted: requires

Deleted: the method requires concatenation with stemflow

Deleted: that are equally or more

Deleted: , and fails to capture potentially significant components of

Deleted: in

Deleted: measurement of which only exacerbates

Deleted: Techniques that yield empirical, site-specific

Deleted: estimates that

Deleted: do so with minimal

Deleted: maintenance and labor

Deleted: estimate total interception (i.e., canopy, understory and litter). Since

Deleted: (here we assume negligible surface runoff due to highly sandy soils in our study sites),

Deleted: is

Deleted: Because

Deleted: to estimate interception was tested forest plots spanning a wide range of conditions (e.g., tree density, composition, groundcover, understory management, age, and hydrogeologic setting) across Florida (USA).

Methods

Estimating Interception Storage Capacity from Soil Moisture Data

During every rainfall event, a portion of the total precipitation (P) is temporarily stored in the forest canopy and groundcover (hereafter referring to both live understory vegetation and forest floor litter). We assume that infiltration (and thus any increase in soil moisture) begins only after total interception storage, defined as the sum of canopy and groundcover storage, is full. We further assume this stored water subsequently evaporates to meet atmospheric demand. Calculating dynamic interception storage requires first determining the total storage capacity (β_s), which is comprised of the storage capacities for the forest canopy (β_c) and groundcover (β_g) (Fig. 1a).

To estimate β_s, we consider a population of individual rainfall events of varying depth over a forest for which high frequency (i.e., 4 hr^{-1}) soil-moisture measurements are available from near the soil surface. Soil moisture content (SMC) at the sensor changes only after rainfall fills total interception storage, evaporative demands since rainfall onset are met, and there is sufficient infiltration for the wetting-front to arrive at the sensor. Rainfall events large enough to induce a soil moisture change (ΔSMC) are evident as a rainfall threshold in the relationship between P and ΔSMC. An example time series of P and SMC (Fig. 1b) yields a P versus ΔSMC relationship (Fig. 1c) with clear threshold behavior. There are multiple equations whose functional forms allow for extraction of this threshold; here we express this relationship as:

$$P = \frac{a}{(1+b*exp^{(-c*\Delta SMC)})} \quad (1)$$

Deleted: array

Deleted: forest

Deleted: A portion of each

Deleted:) (Fig. 1a

Deleted: increases

Deleted: forest

Deleted: , and that

Deleted: Calculation of

Deleted: then

Deleted: maximum

Deleted:), which are added to define total storage capacity (β_s

Deleted: magnitude. Between

Deleted: the

Deleted:

Deleted: reaching a

Deleted: an observed

Deleted: (ΔSMC), interception storages β_c and β_g become saturated. Only rainfall events large enough to overcome this combined storage induce a soil moisture change, with this

Deleted: evident

Deleted: across events.

Deleted: near-surface soil moisture content (

Deleted:)

Deleted: vs.

Deleted: that clearly exhibits this

Deleted: , expressed as:

where P is the total rainfall event depth, ΔSMC is the corresponding soil moisture change, and a, b, and c are fitted parameters. Figure 2 illustrates this relationship and model fitting for observed *SMC* data from six plots at one of our study sites described below. The x-intercept of Eq. 1 (i.e., where *ΔSMC* departs from zero) is given by:

$$P_s = \frac{a}{(1+b)} \qquad (2)$$

Empirically observed values of P_s represent the total rainfall required to saturate β_S, meet evaporative demands between storm onset and observed *ΔSMC*, and supply any infiltration required to induce soil moisture response once interception storage has been saturated. This equality can be expressed as:

$$P_s = \beta_s + \int_0^T Edt + \int_t^T fdt = \beta_s + \int_0^t Edt + \int_t^T Edt + \int_t^T fdt \qquad (3)$$

where T is the total time from rainfall onset until observed change in SMC (i.e., the wetting front arrival), t is the time when β_S is satisfied, and E and f are infiltration and evaporation rates, respectively. To connect this empirical observation to existing analytical frameworks (e.g., Gash 1979), we adopt the term P_G, defined as the rainfall depth needed to saturate β_S and supply evaporative losses between rainfall onset ($t = 0$) and β_S saturation ($t = \mathrm{t}$):

$$P_G = \beta_s + \int_0^t Edt \qquad (4)$$

Solving for β_S in Eq. 3 and substituting into Eq. 4 yields:

$$P_G = P_s - \int_t^T Edt - \int_t^T fdt \qquad (5)$$

Equation 5 may be simplified by assuming that average infiltration and evaporation rates apply during the relatively short period between t and T, such that:

$$P_G = P_s - \acute{f}(T-t) - \acute{E}(T-t) \qquad (6)$$

Deleted: represents rainfall required (P_s) to both saturate total storage capacity ($\beta_s = \beta_c + \beta_g$) and to meet evaporation demand that occurs between rainfall onset and the soil moisture response

Deleted:

where $\acute{f}$ is the average soil infiltration rate and $\acute{E}$ is the average rate of evaporation from the forest surface (i.e., canopy, groundcover, and soil) during the time from *t* to *T* (see Gash 1979). The storage capacity β_s can now be calculated following Gash (1979) as:

$$\beta_s = -P_G \frac{\acute{E}}{\bar{R}} ln\left(1 - \frac{\acute{E}}{\bar{R}}\right) = \frac{-\acute{E}}{\acute{R}} \frac{[P_s - (T-t)(\acute{f}+\acute{E})]}{ln\left(1-\frac{\acute{E}}{\bar{R}}\right)} \quad (7)$$

where $\bar{R}$ is the rainfall rate and all other variables are as previously defined. In Eq. 5, $\acute{E}$ is usually estimated using the Penman-Monteith equation [*Monteith,* 1965] setting canopy resistance to zero (e.g., Ghimire et al 2017).

A key challenge in applying Eq. 5, and thus for the overall approach, is quantifying infiltration, since the time, *t*, when P_G is satisfied is unknown. Moreover, the infiltration rate embedded in P_s is controlled by the rainfall rate ($\bar{R}$) and initial soil moisture content (θ_i). It is worth noting that shallower sensor depth placement would likely eliminate the need for this step (see Discussion). However, to overcome this limitation in our study, we used the 1-D unsaturated flow model HYDRUS-1D (Simunek et al., 1995) to simulate the time it takes for the wetting front to arrive (T_w) at the sensor under bare soil conditions across many combinations of $\bar{R}$ and θ_i. As such, T_w represents the time required for a soil moisture pulse to reach the sensor once infiltration begins (i.e., after total interception capacity has been filled), which is *T*- *t* in Eq. 7. For each simulation, T_w (signaled by the first change in *SMC* at sensor depth) was recorded and used to develop a statistical model of T_w as a function of $\bar{R}$ and θ_i. We used plot-specific soil moisture retention parameters from Florida Soil Characterization Retrieval System (https://soils.ifas.ufl.edu/flsoils/) to develop these curves for our six sites, but simulations can be applied for any soil with known or estimated parameters.

Simulations revealed that T_w at a specific depth declined exponentially with increasing θ_i:

$$T_w = ae^{-b\theta_i} \quad (8)$$

Deleted: P_s can be used to calculate β_s by accounting for rain event evaporation following Gash [1979]:

$$\beta_s = -P_s \frac{\bar{E}}{\bar{R}} \ln\left(1 - \frac{\bar{E}}{\bar{R}}\right) \quad (3)$$

where, $\bar{E}$ and

Deleted: are the mean evaporation rate from wetted surfaces (e.g., vegetation and litter surfaces) and rainfall rates during the rainfall event. $\bar{E}$ is

Deleted: ,

Deleted: [*Monteith,* 1965]. Note that β_s in Eq.3 also includes the moisture stored in the soil column between the where a and b are fitting parameters. Moreover, the parameters a and b in Eq. (6) are well fitted by a power function of $\bar{R}$:

$$a = a_1 \acute{R}^{a_2}, b = b_1 \acute{R}^{b_2} \quad (9)$$

where a_1 and b_1 are fitting parameters. These relationships are illustrated in Fig. 3 for a loamy sand across a range of $\bar{R}$ and θ_i. The relationship between initial *SMC* and T_w is very strong for small to moderate $\bar{R}$ (< 3.0 cm/hr). At higher values of $\bar{R}$, T_w is smaller than the 15-minute sampling resolution, and these events were excluded from our analysis (see below).

Assuming that f equals $\bar{R}$ over the initial infiltration period from t to T (robust for most soils, see below), Eq. 7 can be modified to:

$$\beta_s = \frac{-\acute{E}}{\acute{R}}\left[\frac{P_s - T_w(\acute{R}+\acute{E})}{ln\left(1-\frac{\acute{E}}{\acute{R}}\right)}\right] \quad (10)$$

This approach assumes no runoff or lateral soil-water flow near the top of the soil profile from time t to T. Except for very fine soils under extremely high $\bar{R}$, this assumption generally holds during early storm phases, before ponding occurs (Mein and Larsen, 1973). Moreover, since our goal is to determine β_s, extreme storms can be omitted from the analysis when implementing Eqs. 1-10, without compromising our estimates. Finally, we note that values of β_s from Eq. 10 represent combined interception from canopy and groundcover, but the method does not allow for disaggregation of these two components.

Calculating Interception Loss

Interception storage and resulting interception loss for a given rain event are driven by both antecedent rain (which fills storage) and evaporation (which depletes it). Instantaneous available storage ranges from zero (saturated) to the maximum capacity (i.e., β_s which occurs when the storage is empty). While discrete, event-based interception models [*Gash,* 1979, 1995; *Liu*, 1998] have been widely applied to estimate interception, continuous models more accurately

Deleted: and the ground surface (see

Deleted: 1a) during the period between rainfall onset and evidence of Δ*SMC*. Where *SMC* measurements are obtained close to the soil surface, this shallow soil storage component is

Moved (insertion) [1]

Deleted: and may be considered part of the interception loss [*Savenije*, 2004]. Values of β_s from Eq. 3 allow modeling of

Deleted: cannot disaggregate into canopy and forest-floor interception losses

Deleted: the

Deleted: largely

Deleted:), where instantaneous

Deleted: are

represent time-varying dynamics in interception storage and losses. We adopted the continuous, physically-based interception modeling framework of *Liu* [1998, 2001]:

$$I = \beta_s(D_0 - D) + \int_0^T (1 - D)Edt \qquad (11)$$

where I is interception, E is the evaporation rate from wetted surfaces, D_0 is the forest dryness index at the beginning of a rain event, and D is the forest dryness index at time T. The dryness index is calculated as:

$$D = 1 - \frac{C}{\beta_s} \qquad (12)$$

where C is "adherent storage" (i.e., water that does not drip to the ground) and is given by:

$$C = \beta_s\left(1 - D_0 exp\left(\frac{-(1-\tau)}{\beta_s}P\right)\right) \qquad (13)$$

where τ is the free throughfall coefficient. Because our formulation of β_s in Eq. 10 incorporates both canopy and groundcover components (i.e., negligible true throughfall), we approximated τ in Eq. 13 as zero. For single storms or when sufficient time has passed to dry the canopy, D_0 is assumed to be unity [*Liu* 2001]. Between rainfall events, water in interception storage evaporates to meet atmospheric demand, until the dryness index, D reaches unity [*Liu* 1997]. The rate of evaporation from wetted surfaces between rainfall events (E_s) is:

$$E_s = E(1 - D_0)exp\left(\frac{E}{\beta_s}\right) \qquad (14)$$

A numerical version of Eq. 9 to calculate interception at each time step, t, is expressed as:

$$I = \beta_s(D_{t-1} - D_t) + \frac{1}{2}[E_{t-1}(1 - D_{t-1}) + E_t(1 - D_t)] \qquad (15)$$

Eq. 15 quantifies continuous and cumulative interception losses using precipitation and other climate data (for E) along with β_s derived from soil moisture measurements and corresponding meteorological data.

Deleted:

Deleted: $\int_0^T (1 - D)\,E\,dt$ (4)

Deleted: and

Deleted: and D are

Deleted: values

Deleted: ,

Deleted: $\frac{C}{\beta_s}$ (5)

Deleted: $D_0 = 1 - \frac{C_0}{\beta_s}$ (6)
and
$C = \beta_s\left(1 - D_0 \exp\left(-\frac{(1-\tau)P}{\beta_s}\right)\right)$ (7)

Deleted: C_o and

Deleted: are

Deleted: at

Deleted: start of rainfall

Deleted: at time T, and

Deleted: a

Deleted: β_s

Deleted: ,

Deleted: 7 is set to

Moved up [1]: Eqs.

Deleted: 4 through 9 assume the same evaporation rate, E for the entire forest surface despite

Deleted: evaporation rates that may be greater than rates on the forest floor [*Gerrits et al.*, 2010]. Because we consider the entire forest surface, not just individual components (i.e., canopy or forest floor), errors due to this assumption are likely

Deleted: small.

Deleted: with

Deleted: one

Deleted: =

Deleted: exp

Deleted: *(8*

Deleted: 4

Deleted:

Deleted: $[E_{t-1}(1 - D_{t-1}) + E_t(1 - D_t)]$ (9

Deleted: 9

Deleted: time series

Study Area and Data

As part of a multi-year study quantifying forest water use under varying silvicultural management, we instrumented six sites across Florida, each with six 2-ha plots spanning a wide range of forest structural characteristics. Sites varied in hydroclimatic forcing (annual precipitation range: 131 to 154 cm/yr and potential *ET* range: 127 to 158 cm/yr) and hydrogeologic setting (shallow vs. deep groundwater table). Experimental plots within sites varied in tree species, age, density, leaf area index (LAI), groundcover density (%GC), soil type, and management history (Table 1). Each site contained a recent clear-cut plot, a mature pine plantation plot, and a restored longleaf pine (*Pinus palustris*) plot; the three remaining plots at each site included stands of slash pine (*Pinus elliottii*), sand pine (*Pinus clausa*), or loblolly pine (*Pinus taeda*) subjected to varying silvicultural treatments (understory management, canopy thinning, prescribed burning) and hardwood encroachment.

Within each plot, three banks of TDR sensors (CS655, Campbell Scientific, Logan, UT, USA) were installed to measure soil moisture at multiple soil depths (Fig. 1a). Only data from the top-most sensor (15 cm below the ground surface) were used in this study. Soil-moisture sensor banks were located to capture representative variation in stand geometry (i.e., below the tree canopy and within inter-canopy rows), and thus capture variation in surface soil moisture response to rainfall events driven by forest canopy and groundcover differences. Within each clear-cut plot at each site, meteorological data (rainfall, air temperature, relative humidity, solar insolation, wind speed and direction) were measured using a weather station (GRSW100, Campbell Scientific, Logan, UT; Fig. 4c) every 3 seconds and used to calculate hourly *E* by setting the canopy resistance to zero [*Ghimire et al.,* 2017; *Gash,* 1995; *Monteith,* 1965]. Growing season forest canopy LAI (m^2 m^{-2}) and groundcover (%) were measured at every 5-m

Deleted: Proof of Concept:

Deleted: enumerating

Deleted: installed

Deleted:

Deleted: Plots

Deleted: .

Deleted: as well as

Deleted: , with

Deleted: including

Deleted: pine subject

Deleted: and

Deleted: Three

Deleted: 5-6

Deleted: soil moisture

Deleted: [

Deleted: Model CS655]

Deleted: in each plot

Deleted: up to 2.5 m. The shallowest sensor at each bank was 15 cm below ground

Deleted:) and provided SMC

Deleted: (15-minute intervals

Deleted: 2014-2016)

Deleted: estimate β_s. A Campbell Scientific GRSW100 weather station installed

Deleted: collected

Deleted: every 3 seconds, which were node within a 50 m x 50 m grid surrounding soil moisture measurement banks. LAI was measured at a height of 1 m using a LI-COR LAI-2200 plant canopy analyzer, and %GC was measured using a 1 m^2 quadrat.

To estimate β_s, mean ΔSMC values from the three surface sensors were calculated for all rainfall events separated by at least 72 hours. Storm separation was necessary to ensure the canopy and groundcover surfaces were mostly dry at the onset of each included rainfall event. Rainfall events were binned into discrete classes by depth and plotted against mean ΔSMC to empirically estimate P_s (e.g., Fig. 2). For each rainfall bin, mean θ_i, $\bar{R}$ and $\bar{E}$ were also calculated to use in Eq. 10, which was then applied to calculate β_s. Subsequently, we developed generalized linear models (GLMs) using forest canopy structure (site-mean LAI), mean groundcover (% GC), hydrogeologic setting (shallow vs. deep groundwater table), and site as potential predictors, along with their interactions, to statistically assess predictors of β_s estimates. Because models differed in fitted parameter number, the best model was selected using the Akaike Information Criteria (AIC; Akaike, 1974). Finally, we calculated cumulative annual interception loss (I_a) and its proportion of total rainfall for each study plot using the mean β_s for each plot (across the 3 sensor banks), climate data from 2014 to 2016, and Eq. 15. All analyses were performed using R statistical software [*R Core Team,* 2017].

Results

Total Storage Capacity (β_s)

The exponential function used to describe the P-ΔSMC relationship (Eq. 1) showed strong agreement with observations at all sites and plots (overall $R^2 = 0.80$; $0.47 \le R^2 \le 0.97$; Table 1) as illustrated for a single site in Fig. 2. This consistency across plots and sites suggests

Deleted: above 1-m

Deleted: while

Deleted: for each bank within every plot, corresponding

Deleted: surface was

Deleted: rain

Deleted: ,

Deleted: then

Deleted: for each depth-class was plotted vs. *P*

Deleted: β_s using Eqs. 1 and 3, respectively. As noted, β_s estimated this way

Deleted: includes water stored in the soil column above the soil moisture sensor (15 cm in this case), likely overestimating derived β_s values. Shallower sensor placement would enable measurement of interception as more traditionally defined (i.e., water not reaching the soil), highlighting the general utility of our approach and its flexibility

Deleted: quantify storage as defined by installation design. ¶ To assess the drivers of β_s estimates, a multiple regression model was

Deleted: the

Deleted: mean antecedent soil water storage (storage at the beginning of rainfall events) in the top-soil (expressed as degree of saturation (S) = SMC/SMC_{max})

Deleted: . For each plot, the antecedent S values were extracted for all the rainfall events that were large enough to satisfy the estimated β_s. The regression model based on S

Deleted: LAI and %GC, therefore, incorporates the effects of all the three components of the forest that drive β_s estimated by Eqs. 1 through 3. In addition to the regression models, a variance component analysis was also performed to understand the variability of β_s at point, plot, and site scales respectively. ¶ ¶ ¶

Deleted: 9, we calculated cumulative annual interception loss (I_a) and its proportion relative to total rainfall for each study plot. Effects of LAI, %GC and other site characteristics on proportional I_a losses were assessed by means of general linear models.

Deleted: the

Deleted:

Deleted: (Eq. 1)

Deleted: mean

Deleted:). Observed and modeled P-ΔSMC relationships

Deleted: the six plots at

Deleted: located in the Florida panhandle (site EF)

Deleted: indicate the range of observed behaviors.

that Eq. 1 is capable of adequately describing observed P-ΔSMC relationships, enabling estimates of β_s across diverse hydroclimatic settings and forest structural variation. Estimates of β_s ranged from 0.01 to 0.62 cm, with a mean of 0.30 cm. Plot-scale LAI was moderately correlated with plot-mean β_s, describing roughly 32% of observed variation across plots (Fig. 4a). This relatively weak association may arise because LAI measurements only characterize canopy cover, while β_s combines canopy and groundcover storage. The best GLM of β_s (Fig. 4b) used %GC and an interaction term between site and LAI (R^2 = 0.84 and AIC = 253.7, Table 2). The best GLM without site used LAI and hydrogeologic setting (shallow vs. deep water table) but had reduced performance (R^2 = 0.55 and AIC = 338.3; Table 2).

Annual Interception Losses (I_a)

Despite having similar rainfall regimes (mean annual precipitation ranging from 131 to 154 cm yr^{-1} across sites), mean annual interception losses (I_a) differed significantly both across sites (one-way ANOVA $p < 0.001$) and among plots within sites (one-way ANOVA $p < 0.001$). Estimates of I_a/P across all plots and sites ranged from 6 to 21% of annual rainfall (Table 1) and were moderately but significantly correlated with mean LAI, explaining approximately 30% of variation in I_a (Fig. 5a). Correlations among I_a/P and LAI were stronger for individual sites than the global relationship ($0.51 \leq R^2 \leq 0.84$), except for site EF, where I_a losses were small and similar across plots regardless of LAI (Fig. 5b; Table 1). This suggests that additional site-level differences (e.g., hydroclimate, soils, geology) play a role in driving I_a, as expected following from their effects on β_s described above.

Discussion and Conclusions

When combined with local rainfall data, near-surface soil moisture dynamics inherently contain information about rainfall interception by above-ground structures. Using soil moisture

Deleted: describes the…observed P-ΔSMC relationships, enablingand thus enables…estimates of β_s across diverse hydroclimatic settings and forest structural variation. ¶ Estimates of β_s ranged from 0.0123 cm…to 0.621.2…cm, with a mean of 0.30 cm. Plot6 cm. However, among the 36 forests plots that were analyzed only 2 had $\beta s \geq 1.0$ cm. Excluding these two plots as outliers resulted in mean β_s = 0.55 cm and maximum βs = 0.96 cm. Estimated β_s values showed increasing variance from the point…scale LAI was moderately(i.e., among the three sensor banks within a plot, CV = 0.18) to the plot scale (i.e., across the six plots within a site, CV = 0.26) to the site scale (i.e., across all measurement locations, CV = 0.47). These results follow from hydroclimatic, edaphic, and vegetation variation, all of which increase with increasing scales of analysis. Indeed, an analysis of the random variance components (Fig. 3a) performed for a general linear mixed model revealed that 43% of the total variance in β_s could be attributed to site differences followed by 33% attributable to plot level differences. Within plots, only 23% of the variance in β_s was attributed to bank differences indicating that estimates of β_s were similar between proximate measurements. Variability in β_s across plots within a site is primarily driven by variation in forest structure (LAI and %GC), which is sensitive to management decisions. Across sites, variability in β_s is driven by both hydroclimatic and management differences that control forest canopy and groundcover composition. The smaller variability in β_s observed at the point scale supports our use of mean plot values (i.e., the mean across three sensor banks) for subsequent analyses. ¶ Across plots, LAI was significantly…correlated with plot-mean β_s, describing roughly 3240… of observed variation across plots (Fig. 4a3b…. This relatively weak association may arise because LAI measurements only characterize canopy cover, while β_s combines canopy and groundcover storage. The best GLM of β_s (Fig. 4b) used %GC and an Multiple linear regression using LAI and %GC increased model explanatory power to 56% of the observed variation in β_s (not shown). We note again that β_s estimates in our ... [1]

Deleted: Annual …ainfall regimes (mean annual precipitation rangingranged…from 131120 cm…to 154160…cm yr^{-1} acrossand diffed significantly among the six…sites),…mM…an annual interception losses (I_a) also differed significantly both acrossamong…sites (one-way ANOVA $p < 0.001$),…and among plots within sites (one-way ANOVA p-value…< 0.001). Estimates of) despite receiving the same rainfall input.…I_a/P estimates…across all plots and sites ranged from 613…to 2128… of annual rainfall (Table 1) and were moderately,showed a moderate…but significantly, correlatedsignificant correlation…with the …ean LAI, explaining approximately 3040… of variation in I_a (Fig. 5a).during the three year study period.…Correlations among between fractions of annual interception loss (…$_a/P$)…and LAI were much …tronger for individual sites than the global relationship (0.5138…$\leq R^2 \leq$ 0.84),95,…except forthe EF…site EF, where the …$_a$ losses were relatively …mall and similar across all…plots regardless of LAI (Fig. 5b; Table 1). This suggests that compared to the other sites, see SI table S2), highlighting. [2]

Deleted: cumulative …ainfall interception by above-ground structures. Using the empirical ... [3]

data, we developed and tested an analytical approach for estimating total interception storage capacity (β_s) that includes canopy, understory, and groundcover vegetation, as well as any litter on the forest floor. The range of β_s given by our analysis (mean $\beta_s = 0.30$ cm; $0.01 \leq \beta_s \leq 0.62$ cm) is close to, but generally higher than previously reported canopy storage capacity values for similar pine forests (e.g., 0.17 to 0.20 cm for mature southeastern USA pine forests; Bryant et al. 2005).

An important distinction between our method and previous interception measurement approaches is that the soil moisture-based method estimates composite rainfall interception of not only the canopy, but also of the groundcover vegetation and forest floor litter. Rainfall storage and subsequent evaporation from groundcover vegetation and litter layers can be as high, or higher than, canopy storage in many forest landscapes [*Putuhena and Cordery,* 1996; *Gerrits et al.,* 2010]. For example, *Li et al.* [2017] found that the storage capacity of a pine forest floor in China was between 0.3 and 0.5 cm, while maximum canopy storage was < 0.1 cm. *Putuhena and Cordery* [1996] also estimated storage capacity of pine forest litter to be approximately 0.3 cm based on direct field measurements. *Gerrits et al.* [2007] found forest floor interception to be 34% of measured precipitation in a beech forest, while other studies have shown that interception by litter can range from 8 to 18% of total rainfall [*Gerrits et al.,* 2010; *Tsiko et al.,* 2012; *Miller et al.,* 1990; *Pathak et al.,* 1985; *Kelliher et al.,* 1992]. A recent study using leaf wetness observations [*Acharya et al.* 2017] found the storage capacity of eastern redcedar (*Juniperus virginiana*) forest litter to range from 0.12 to as high as 1.12 cm, with forest litter intercepting approximately 8% of gross rainfall over a six-month period. Given the composite nature of forest interception storage and the range of storage capacities reported in these studies, the values we report appear to be plausible, and consistent with the expected differences between canopy-only

Deleted: the "whole-forest"

Deleted: layers. Our estimates

Deleted: ranged from 0.23 cm to 1.2 cm, with a

Deleted: value of

Deleted: 6 cm. These values are considerably

Deleted: capacities reported in the literature

Deleted: regional forest types

Deleted: 2

Deleted: 2005]. However, our estimates also include important groundcover storage, along with the shallow soil storage (0-15 cm), yielding higher overall storage capacity values. While shallower installation of soil-moisture sensors (e.g., 0 - 5 cm depth) would reduce top-soil storage fractions in β_s, results here highlight the general applicability our approach and provide robust inferences regarding management and hydroclimatic drivers of forest interception.

Deleted: Collective rainfall storage by ground cover

Deleted: 2010], necessitating enumeration for accurate water budgets.

Deleted: In another recent study, *Acharya et al* [2017] found, using the leaf wetness observations, that the storage capacity of forest litter of an eastern redcedar forest ranged from 0.12 to 1.12 cm and the forest litter intercepted ca. 8% of gross rainfall during a 6-month period.

Deleted: ca.

and total interception storage. As such, our results support the general applicability of the soil moisture-based approach for developing forest interception estimates across a wide range of hydroclimatic and forest structural settings.

Interception losses vary spatially and temporally and are driven by both β_s and climatic variation (i.e., P and E). Our approach represents storage dynamics by combining empirically derived β_s estimates with climatic data using a previously developed continuous interception model [*Liu* 1998, 2001]. Cumulative I_a estimates in this study ranged considerably (i.e., from 6% to 21% of annual rainfall) across the 34 plots, which were characterized by variation in canopy structure ($0.12 < \mathrm{LAI} < 3.70$) and groundcover ($7.9 < \%\mathrm{GC} < 86.2$). In comparison, interception losses by pine forests reported in the literature (all of which report either canopy-only or groundcover-only values, but not their composite) range from 12 to 49% of incoming rainfall [*Bryant et al.*, 2005; *Llorens et al.*, 1997; *Kelliher and Whitehead*, 1992; *Crockford and Richardson*, 1990]. Notably, most of the variation in this range is drive by climate rather than forest structure, with the highest I_a values from more arid regions (e.g., Llorens et al. 1997). Broad agreement between our results and literature I_a values supports the utility of our method for estimating this difficult-to-measure component of the water budget. Additionally, the magnitude and heterogeneity of our I_a estimates across a single forest type (southeastern US pine) underscores the urgent need for empirical measurements of interception that incorporate information on both canopy and groundcover storage in order to develop accurate water budgets. This conclusion is further bolstered by the persistent importance of site-level statistical effects in predicting β_s (and therefore I_a), even after accounting for forest structural attributes, which suggests there are influential edaphic or structural attributes that we are not currently adequately assessing.

Deleted: Given the composite nature of forest interception storage capacity considered, values reported here appear entirely plausible.
Deleted: e
Deleted: varying,
Deleted: in
Deleted: integrating
Deleted: .
Deleted: 36
Deleted: (13% -28% of rainfall),
Deleted: a
Deleted: a wide range of
Deleted: 7
Deleted: 5.0
Deleted: 90.0
Deleted: total canopy
Deleted: range
Deleted: This broad
Deleted: with values from the
Deleted: reasonably
Deleted: interception losses, despite generally higher estimates of β_s. The
Deleted: SE
Deleted: this component of the water budget, a
Deleted: I_a,
Deleted: .

Generally, estimated I_a losses in clear-cut plots were smaller than plots with a developed canopy, as expected. One exception was at EF where the clear-cut plot exhibited the highest I_a of the six EF plots (8.4%, Table 1). Notably, differences among EF plots were very small (I_a ranged only from 7.9 to 8.4 % of annual rainfall), an annual interception rate consistent with or even slightly lower than other clear cuts across the study. This site is extremely well drained and has dense litter dominated by mosses and nutrient-poor sandy soils, highlighting the potential for additional local measurements to better understand how forest structure controls observed interception.

There are several important methodological considerations and assumptions inherent to estimating interception using near-surface soil moisture data. First is the depth at which SMC is measured. Ideally, soil moisture would be measured a few centimeters into the soil profile, eliminating the need to account for infiltration when calculating P_G in Eqs. (4-6). Soil moisture data used here were leveraged from a study of forest water yield, with sensor deployment depths selected to efficiently integrate soil moisture patterns through the vadose zone. While the extra step of modeling infiltration may increase uncertainty in β_s, infiltration was extremely well-described using wetting front simulations of arrival time based on initial soil moisture and rainfall. As such, while we advocate for shallower sensors in future efforts, our solution here given the depths that were available seem tenable for this and other similar data sets. Second, in contrast to the original Gash (1979) formulation, Eq. 5 does not explicitly include throughfall. While throughfall has been a critical consideration for rainfall partitioning by the forest canopy, our approach considers total interception by aboveground forest structures (canopy, groundcover, and litter). A portion of canopy throughfall is captured by non-canopy storage and thus intercepted. Constraining this fraction is not possible with the data available, and indeed our soil moisture response reflects the "throughfall" passing the canopy, understory and litter. Similarly, estimation of β_s using Eqs. 1-7 cannot directly account for stemflow, which can be an important component of rainfall partitioning in forests (e.g., Bryant et al., 2005). We used the mean soil moisture response across three sensor locations (close to a tree, away from the tree but below the canopy, and within inter-canopy rows), which lessens the impact of this assumption on our estimates of β_s. Finally, Eqs. (3-10) assume the same evaporation rate, E, for intercepted water from the canopy and from the understory. Evaporation rates may vary substantially between the canopy, understory, and forest floor [*Gerrits et al.*, 2007, 2010], especially in more energy-limited environments. Future work should consider differential evaporation rates within each interception storage, particularly since the inclusion of litter as a component potentially accentuates these contrasts in E.

Rainfall interception by forests is a dynamic process that is strongly influenced by rainfall patterns (e.g., frequency, intensity), along with various forest structural attributes such as interception storage capacity (β_s) [*Gerrits et al.*, 2010]. In this work, we coupled estimation of a total (or "whole-forest") β_s parameter with a continuous water balance model [*Liu,* 1997, 2001; *Rutter et al.,* 1975], providing an integrative approach for quantifying time-varying and cumulative interception losses. We propose that soil moisture-based estimates of β_s have the potential to more easily and appropriately represent combined forest interception relative to existing time- and labor-intensive field methods that fail to account for groundcover and litter interception. Soil moisture can be measured relatively inexpensively and easily using continuous logging sensors that require little field maintenance, facilitating application of the presented approach across large spatial and temporal extents and reducing the time and resources that are needed for other empirical measures [e.g., *Lundberg et al.,* 1997]. Finally, while direct

Deleted: Generally, interception in clear-cut plots was smaller than other plots with a forest canopy. However, a few clear-cut plots intercepted as much rainfall as nearby forested plots (See SI Table S2). . This may be attributed to the dense groundcover vegetation that rapidly establishes in clear-cut plots following tree removal and attendant increases in both water and light availability. For example, at the Green Swamp (GS) site, %GC in the clear-cut plot increased from < 10% at the beginning of the study (few weeks after clearing in July 2014) to ca. 90% near the end of the study period (attributed entirely to rapidly growing grasses and low-stature woody shrubs). On average, 23% of incoming rainfall was lost to interception during the three-year period. In contrast, several plots with pine canopies, but with substantially lower %GC, had lower or similar values of I_a. We note that both canopy and understory structure impact interception, but that there is a strong negative association between LAI and %GC across plots (See SI Table S2). As such, interception variation across plots with starkly different canopy structure was lower than expected. ¶
As noted above, a critical factor that affects estimation of β_s (and hence I_a) from near-surface soil moisture data is the depth of SMC measurement. Although SMC measurement at the top of the soil-profile (i.e., within the first few centimeters of soil) may be ideal, our SMC observations (at 15 cm) were from a larger project. Accordingly, β_s values obtained using Eq (1) likely overestimate the actual storage capacity. Installing sensors at the shallowest possible depth may minimize this error, though it remains unclear whether between-sensor variation will be as low when sampling very shallow soils. We note that errors in I_a due to soil storage are likely to be relatively small because the majority of rainfall events are smaller than β_s. Moreover, shallow soil depths wetted during rainfall may also contribute to interception since the moisture retained is more likely to return to the atmosphere via evaporation than contribute to plant transpiration [*Savenije*, 2004]. This is particularly important in warm regions where the collective storage by shallow soil, litter, and groundcover and subsequent wet-surface evaporation are likely greater than what may occur from the forest canopy alone. ¶
Rainfall interception by forests is a dynamic process that is most

Deleted:) among

Deleted: factors, including the

Deleted: Therefore, coupling the composite

Deleted: es

Deleted: -

Deleted: . Soilcomparisons with other empirical measures of forest canopy interception should be treated cautiously, this approach yields values that are broadly consistent with the literature, and provide an estimate of combined canopy and groundcover storage capacity that has the potential to improve the accuracy of water balances models at scales from the soil column to watershed

References

Acharya, B.S., Stebler, E., and Zou, C.B.: Monitoring litter interception of rainfall using leaf wetness sensor under controlled and field conditions. *Hydrological Processes,* 31, 240-249: DOI 10.1002/hyp.11047, 2005

Benyon, R.G., Doody, and T. M.: Comparison of interception, forest floor evaporation and transpiration in *Pinus radiata* and *Eucalyptus globulus* plantations. *Hydrological Processes* **29** (6): 1173–1187 DOI: 10.1002/hyp.10237, 2015

Bryant, M.L., Bhat, S., and Jacobs, J.M.: Measurements and modeling of throughfall variability for five forest communities in the southeastern US. *Journal of Hydrology*, DOI: 10.1016/j.jhydrol.2005.02.012, 2005

Bulcock, H.H., and Jewitt, G.P.W.: Modelling canopy and litter interception in commercial forest plantations in South Africa using the Variable Storage Gash model and idealised drying curves. *Hydrol. Earth Syst. Sci* **16**: 4693–4705 DOI: 10.5194/hess-16-4693-2012, 2012

Carlyle-Moses, D.E., and Price, A.G.: Modelling canopy interception loss from a Mediterranean pine-oak stand, northeastern Mexico. *Hydrological Processes* **21** (19): 2572–2580 DOI: 10.1002/hyp.6790, 2007

Carlyle-Moses, D.E., and Gash, J.H.C.: Rainfall Interception Loss by Forest Canopies. *In* Carlyle-Moses and Tanaka (Eds), *Ecological Studies* 216. DOI: 10.1007/978-94-007-1363, 2011

Crockford, R.H., and Richardson, D.P.: Partitioning of rainfall into throughfall, stemflow and interception: effect of forest type, ground cover and climate. *Hydrological Processes* **14** (16–17): 2903–2920 DOI: 10.1002/1099-1085(200011/12)14:16/17<2903::AID-HYP126>3.0.CO;2-6, 2000

Gash, J.H.C., Lloyd, C.R., and Lachaud, B. G.: Estimating sparse forest rainfall interception with an analytical model. *Journal of Hydrology* **170**: 79–86, 1995

Gash, J.H.C.: An analytical model of rainfall interception by forests. *Quarterly Journal of the Royal Meteorological Society* **105** (443): 43–55 DOI: 10.1002/qj.49710544304, 1979

- **Deleted:** Additionally
- **Deleted:** provides a combined
- **Deleted:** and thus "whole-forest" rainfall interception
- **Deleted:** E.
- **Deleted:** C.B.
- **Deleted:** . 2017.
- **Deleted:** . Doody. 2015.
- **Deleted:** S.
- **Deleted:** J.M.
- **Deleted:** . 2005.
- **Deleted:** G.P.W.
- **Deleted:** . 2012.
- **Deleted:** A.G.
- **Deleted:** . 2007.
- **Deleted:** . Gash. 2011.
- **Deleted:** D.P.
- **Deleted:** . 2000.
- **Deleted:** C.R.
- **Deleted:** B. G.
- **Deleted:** . 1995.
- **Deleted:** . 1979.

Gerrits, A.M.J., Savenije, H.H.G., Hofmann, L., and Pfister, L.: New technique to measure forest floor interception – an application in a beech forest in Luxembourg. *Hydrol. Earth Syst. Sci* **11**: 695–701, 2007

Ghimire, C.P., Bruijnzeel, L.A., Lubczynski, M.W., and Bonell, M.: Rainfall interception by natural and planted forests in the Middle Mountains of Central Nepal. *Journal of Hydrology* **475**: 270–280 DOI: 10.1016/j.jhydrol.2012.09.051, 2012

Ghimire, C.P., Bruijnzell, L.A., Lubczynski, M.W., Ravelona, M., Zwartendijk, B.W., and Meervald, H.H.: Measurement and modeling of rainfall interception by two differently aged secondary forests in upland eastern Madagascar, Journal of Hydrology, DOI: 10.1016/j.jhydrol.2016.10.032, 2017

Liu, J.: A theoretical model of the process of rainfall interception in forest canopy. *Ecological Modelling* **42**: 111–123, 1988

Kelliher, F.M., Whitehead, D., and Pollock D.S.: Rainfall interception by trees and slash in a young Pinus radiata D. Don stand. *Journal of Hydrology* **131** (1–4): 187–204 DOI: 10.1016/0022-1694(92)90217-J, 1992

Li, X., Xiao, Q., Niu, J., Dymond, S., Mcherson, E. G., van Doorn, N., Yu, X., Xie, B., Zhang, K., and Li, J.: Rainfall interception by tree crown and leaf litter: an interactive process. *Hydrological Processes* DOI: 10.1002/hyp.11275, 2017

Liu, S.: Evaluation of the Liu model for predicting rainfall interception in forests world-wide. *Hydrological Processes* **15** (12): 2341–2360 DOI: 10.1002/hyp.264, 2001

Liu, S.: A new model for the prediction of rainfall interception in forest canopies. *Ecological Modelling* **99**: 15–159, 2001

Liu, S.: Estimation of rainfall storage capacity in the canopies of cypress wetlands and slash pine uplands in North-Central Florida. *Journal of Hydrology* **207**: 32–41, 1998

Llorens, P., and Poch, R.: Rainfall interception by a *Pinus sylvestris* forest patch overgrown in a Mediterranean mountainous abandoned area I. Monitoring design and results down to the event scale. *Journal of Hydrology* **199**: 331–345, 1997

Lundberg, A., Eriksson, M., Halldin, S., Kellner, E., and Seibert, J.: New approach to the measurement of interception evaporation. Journal of Atmospheric and Oceanic Technology 14 (5), 1023–1035, 1997

Massman, W.J.: The derivation and validation of a new model for the interception of rainfall by forests. *Agricultural and Forest Meteorology* **28**: 261–286, 1983

Merriam, R.A.: A note on the interception loss equation. *Journal of Geophysical Research* **65** (11): 3850–3851 DOI 10.1029/JZ065i011p03850, 1960

Deleted: H.H.G.
Deleted: . Hoffmann,
Deleted: L.
Deleted: . 2007.
Deleted: L.A.
Deleted: M.W.
Deleted: M.
Deleted: . 2012.
Deleted: . Bruijnzeel, M.W.
Deleted: B.W.
Deleted: . Meerveld. 2017.
Deleted: . 1988.
Deleted: D.
Deleted: D.S.
Deleted: . 1992.
Deleted: Q.
Deleted: J.
Deleted: S.
Deleted: . McPherson, N.
Deleted: X.
Deleted: B.
Deleted: K.
Deleted: J.
Deleted: . 2017.
Deleted: . 2001.
Deleted: . 1997.
Deleted: . 1998.
Deleted: *Journal*
Deleted: R.
Deleted: . 1997.
Deleted: g
Deleted: M.
Deleted: S.
Deleted: E.
Deleted: J.
Deleted: .1997.
Deleted: .
Deleted: . 1983.
Deleted: . 1960.
Deleted: :

Muzylo, A., Llorens, P., Valente, F., Keizer, J.J., Domingo, F., and Gash, J.H.C. Gash. A review of rainfall interception modelling. *Journal of Hydrology* **370**: 191–206 DOI: 10.1016/j.jhydrol.2009.02.058, 2009

Pook, E.W., Moore, P.H.R., and Hall, T.: Rainfall interception by trees of *Pinus radiata* and *Eucalyptus viminali* in a 1300 mm rainfall area of southeastern New South Wales: I. Gross losses and their variability. *Hydrological Processes* **5** (2): 127–141 DOI: 10.1002/hyp.3360050202, 1991

Putuhena, W.M., and Cordery, I.: Estimation of interception capacity of the forest floor. *Journal of Hydrology* **180**: 283–299, 1996

Rutter, A.J., Morton, A.J., and Robins, P.C.: A Predictive Model of Rainfall Interception in Forests. II. Generalization of the Model and Comparison with Observations in Some Coniferous and Hardwood Stands *Journal of Applied Ecology* **12** (1): 367–380, 1975

Savenije, H. H. G.: The importance of interception and why we should delete the term evapotranspiration from our vocabulary, Hydrol. Processes, 18, 1507 – 1511, 2004

Schaap, M.G., Bouten, W., and Verstraten, J.M.: Forest floor water content dynamics in a Douglas fir stand. *Journal of Hydrology* **201**: 367–383, 1997

Valente, F., David, J.S., and Gash, J.H.C.: Modelling interception loss for two sparse eucalypt and pine forests in central Portugal using reformulated Rutter and Gash analytical models. *Journal of Hydrology ELSEVIER Journal of Hydrology* **190**: 141–162, 1997

Van Dijk, A.I.J.M., and Bruijnzeel, L.A.: Modelling rainfall interception by vegetation of variable density using an adapted analytical model. Part 1. Model description. Journal of Hydrology, 247:230-238, 2001

Wei, Z., Yoshimura, K., Wang, L., Miralles, D.G., Jasechko, S., and Lee, X.: Revisiting the contribution of transpiration to global terrestrial evapotranspiration. *Geophysical Research Letters* **44** (6): 2792–2801 DOI: 10.1002/2016GL072235, 2017

Xiao, Q., McPherson, E.G., Ustin, S.L., and Grismer, M.E.: A new approach to modeling tree rainfall interception. *Journal of Geophysical Research: Atmospheres* **105** (D23): 29173–29188 DOI: 10.1029/2000JD900343, 2000

Deleted: P.
Deleted: F.
Deleted: J.J.
Deleted: F.
Deleted: P.H.R.
Deleted: T.
Deleted: . 1991.
Deleted: I.
Deleted: . 1996.
Deleted: A.J.
Deleted: P.C.
Deleted: . 1975.
Deleted: . (2004),
Deleted: .
Deleted: W.
Deleted: J.M.
Deleted: . 1997.
Deleted: J.S.
Deleted: . Gash. 1997.
Deleted: L.A.
Deleted: . 2001.
Deleted: K.
Deleted: L.
Deleted: D.G.
Deleted: S.
Deleted: X.
Deleted: . 2017.
Deleted: E.G.
Deleted: S.L.
Deleted: M.E.
Deleted: . 2000.

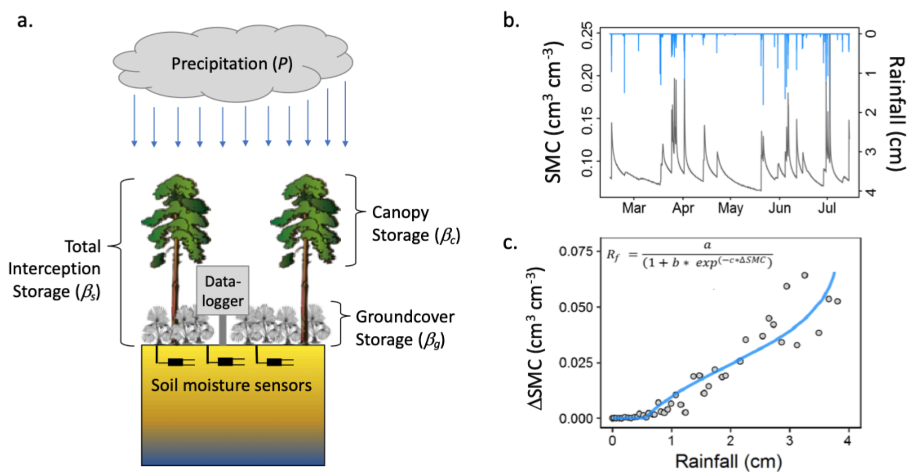

Figure 1. (a) Schematic illustration of experimental setup and interception water storages, where total interception storage (β_s) is the sum of canopy storage (β_c) and groundcover (understory and litter) storage (β_g). (b) Example time series of rainfall (blue lines) and corresponding near-surface soil moisture content (*SMC*, black line; observed at 15 cm in this study). (c) Resultant relationship between rainfall and change in soil moisture *ΔSMC* during rainfall, along with fitted model to extract the x-intercept (i.e., P_s).

Deleted: Page Break
Figure Captions

Deleted: the different

Deleted: during rainfall events,

Deleted: -

Deleted: data (

Deleted: ; black line),

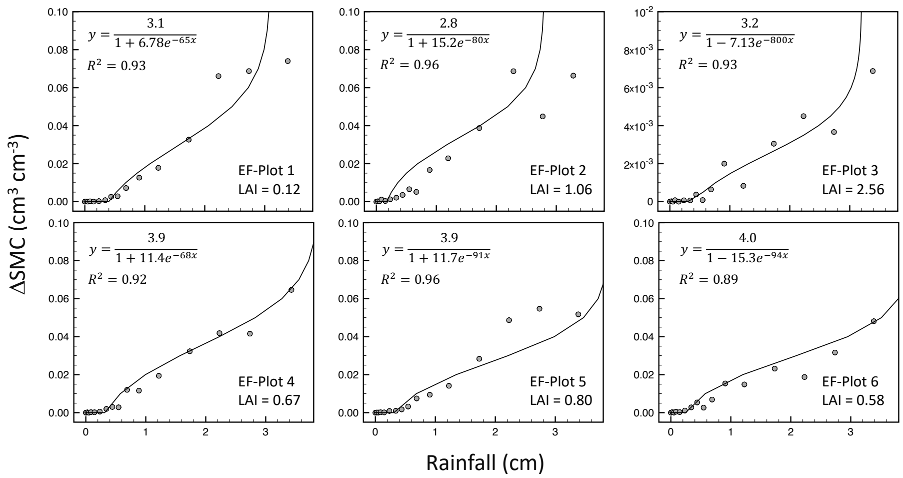

Figure 2: Change in soil moisture content (ΔSMC) versus binned rainfall depths for six plots at one of the study sites used in the study (Econfina; EF). The x-intercept of the fitted relationships were used to derive P_s in Eq. 2. Note different y-axis scale for EF-Plot 3.

Deleted: vs cumulative

Deleted: , where LAI increases with plot number.

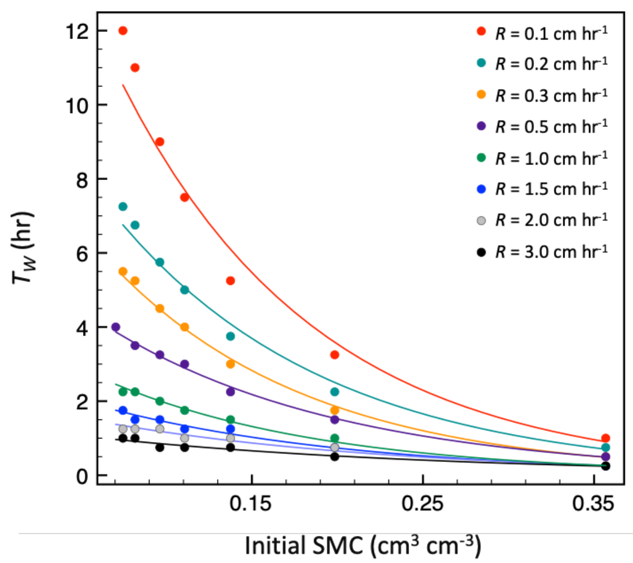

Figure 3: Initial soil moisture content (SMC) versus time of wetting front arrival (T_w) for a loamy sand soil. Dots are simulated results from HYDUS-1D simulation, and lines are the exponential model given in Eq. 8, fitted for each rainfall rate, R.

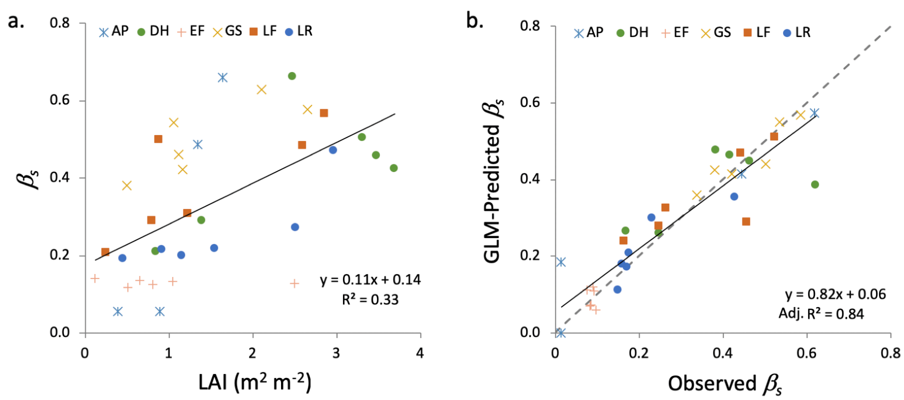

Figure 4. (a) Interception storage capacity (β_s) versus leaf area index (LAI) for all sites and plots. (b) Modeled versus observed β_s using the best GLM, which included % groundcover vegetation and an interaction term between site and LAI. The dashed line is the 1:1 line.

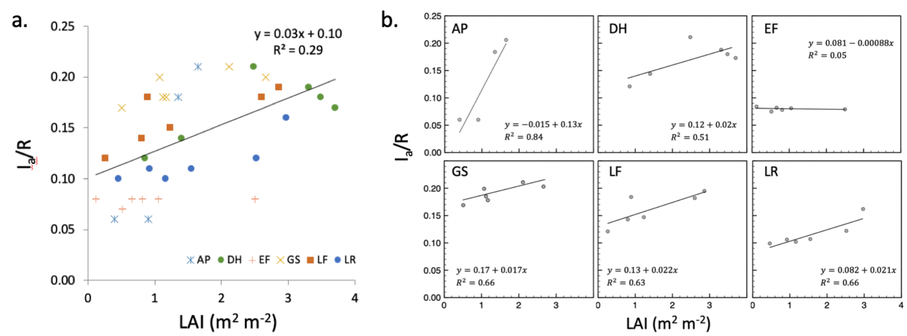

Figure 5. (a) Annual proportion of rainfall that is intercepted (I_a/R) intercepted versus LAI for all sites and plots. (b) Site-specific I_a/R versus LAI relationships. The relationship is generally strong except for the EF site, where the overall storage capacity is small across all values of LAI.

Deleted: denotes P_s (Eq. 2).

Table 1. Summary of storage capacity (β_s) and annual interception losses (I_a) for all sites and plots, along with plot characteristics (mean annual precipitation, P; leaf area index, LAI; percent groundcover, %GC; and species). Note that the AP site only had three plots with the data required for the analysis.

Site	Plot	LAI	%GC	Species	β_s (cm)	R^2 (ΔSMC-R)	P (cm)	I_a/P
AP	2	1.65	47.6	SF Slash	0.620	0.31	145.0	0.206
AP	3	0.90	62.8	SF Slash	0.014	0.78	145.0	0.06
AP	4	1.35	49.1	SF Slash	0.445	0.67	145.0	0.184
AP	6	0.40	73.4	Longleaf	0.014	0.57	145.0	0.06
DH	1	0.85	86.2	Loblolly	0.170	0.90	131.5	0.121
DH	2	2.48	51.2	Slash	0.621	0.68	131.5	0.211
DH	3	1.40	39.2	Slash	0.249	0.49	131.5	0.144
DH	4	3.31	35.8	Slash	0.464	0.71	131.5	0.188
DH	5	3.70	27.1	Loblolly	0.383	0.69	131.5	0.173
DH	6	3.48	32.9	Slash	0.418	0.40	131.5	0.18
EF	1	0.12	13.6	Clearcut	0.099	0.93	153.8	0.084
EF	2	1.05	56.9	Slash	0.092	0.96	153.8	0.081
EF	3	2.50	11.8	Sand	0.086	0.93	153.8	0.079
EF	4	0.66	50.9	Slash	0.094	0.92	153.8	0.082
EF	5	0.81	17.9	Sand	0.085	0.96	153.8	0.078
EF	6	0.52	52.0	Longleaf	0.076	0.89	153.8	0.075
GS	1	1.07	67.9	Clearcut	0.502	0.84	132.4	0.199
GS	2	2.66	7.9	Slash	0.535	0.88	132.4	0.203
GS	3	2.11	71.5	Slash	0.587	0.82	132.4	0.211
GS	4	1.12	42.4	Slash	0.421	0.90	132.4	0.185
GS	5	1.17	45.6	Slash	0.382	0.76	132.4	0.178
GS	6	0.51	55.2	Longleaf	0.339	0.78	132.4	0.169
LF	1	0.26	43.5	None	0.166	0.85	136.3	0.121
LF	2	2.86	23.1	Slash	0.525	0.64	136.3	0.195
LF	3	1.23	24.9	Slash	0.266	0.72	136.3	0.147
LF	4	0.80	25.7	Slash	0.248	0.64	136.3	0.143
LF	5	2.60	12.3	Slash	0.443	0.63	136.3	0.182
LF	6	0.89	25.9	Longleaf	0.458	0.69	136.3	0.184
LR	1	0.46	34.0	Clearcut	0.151	0.96	144.5	0.099
LR	2	2.97	38.1	Slash	0.429	0.84	144.5	0.162
LR	3	0.92	47.0	Slash	0.173	0.95	144.5	0.106
LR	4	2.52	26.7	Slash	0.232	0.92	144.5	0.122
LR	5	1.55	28.1	Slash	0.177	0.96	144.5	0.107
LR	6	1.16	35.5	Longleaf	0.160	0.96	144.5	0.102

Table 2. Summary of generalized linear model (GLM) results for interception storage capacity (β_s). LAI is leaf area index, GC is groundcover, and WT is water table (shallow vs. deep). The best model (by AIC) is shown in bold.

Model #	Variable(s)	AIC	R^2
1	LAI	378.1	0.32
2	LAI + site	318.5	0.66
3	LAI * site	255.9	0.83
4	**LAI * site + GC**	**253.1**	**0.84**
5	LAI + WT	338.3	0.55
6	LAI * WT	339.8	0.55
7	LAI * WT + GC	341.8	0.55
8	LAI + WT + GC	340.3	0.55

Deleted: Figure 3: (a) Components of the total observed variances in β_s at bank, plot and site scales, and b) LAI vs mean β_s for all plots across all sites.
Figure 4: a) Observed β_s versus the predicted β_s values from the multiple linear regression model with LAI, groundcover and antecedent soil wetness predictors, and b) Observed I_a/P vs predicted I_a/P from the linear mixed-effect model with random site level effects. The gray line indicates 1:1 line and the blue line is the best fit.

Demonstration of a simple method to estimate rainfall interception by forests using near-surface soil moisture responses is presented
The method provides composite estimates of total interception by the canopy, understory, groundcover vegetation and forest floor litter
The method is potentially more feasible to apply at larger spatiotemporal extents compared to previous approaches.

Page 12: [1] Deleted	Acharya,Subodh	5/9/19 10:11:00 AM

Page 12: [1] Deleted	Acharya,Subodh	5/9/19 10:11:00 AM

Page 12: [1] Deleted	Acharya,Subodh	5/9/19 10:11:00 AM

Page 12: [1] Deleted	Acharya,Subodh	5/9/19 10:11:00 AM

Page 12: [1] Deleted	Acharya,Subodh	5/9/19 10:11:00 AM

Page 12: [1] Deleted	Acharya,Subodh	5/9/19 10:11:00 AM

Page 12: [1] Deleted	Acharya,Subodh	5/9/19 10:11:00 AM

Page 12: [1] Deleted	Acharya,Subodh	5/9/19 10:11:00 AM

Page 12: [1] Deleted	Acharya,Subodh	5/9/19 10:11:00 AM

Page 12: [1] Deleted	Acharya,Subodh	5/9/19 10:11:00 AM

Page 12: [1] Deleted	Acharya,Subodh	5/9/19 10:11:00 AM

Page 12: [1] Deleted	Acharya,Subodh	5/9/19 10:11:00 AM

Page 12: [2] Deleted Acharya,Subodh 5/9/19 10:11:00 AM

Page 12: [2] Deleted Acharya,Subodh 5/9/19 10:11:00 AM

Page 12: [2] Deleted Acharya,Subodh 5/9/19 10:11:00 AM

Page 12: [2] Deleted Acharya,Subodh 5/9/19 10:11:00 AM

Page 12: [2] Deleted Acharya,Subodh 5/9/19 10:11:00 AM

Page 12: [2] Deleted Acharya,Subodh 5/9/19 10:11:00 AM

Page 12: [2] Deleted Acharya,Subodh 5/9/19 10:11:00 AM

Page 12: [2] Deleted Acharya,Subodh 5/9/19 10:11:00 AM

Page 12: [2] Deleted Acharya,Subodh 5/9/19 10:11:00 AM

Page 12: [2] Deleted Acharya,Subodh 5/9/19 10:11:00 AM

Page 12: [2] Deleted Acharya,Subodh 5/9/19 10:11:00 AM

Page 12: [2] Deleted Acharya,Subodh 5/9/19 10:11:00 AM

Page 12: [2] Deleted	Acharya,Subodh	5/9/19 10:11:00 AM

Page 12: [2] Deleted	Acharya,Subodh	5/9/19 10:11:00 AM

Page 12: [2] Deleted	Acharya,Subodh	5/9/19 10:11:00 AM

Page 12: [2] Deleted	Acharya,Subodh	5/9/19 10:11:00 AM

Page 12: [2] Deleted	Acharya,Subodh	5/9/19 10:11:00 AM

Page 12: [2] Deleted	Acharya,Subodh	5/9/19 10:11:00 AM

Page 12: [2] Deleted	Acharya,Subodh	5/9/19 10:11:00 AM

Page 12: [2] Deleted	Acharya,Subodh	5/9/19 10:11:00 AM

Page 12: [2] Deleted	Acharya,Subodh	5/9/19 10:11:00 AM

Page 12: [2] Deleted	Acharya,Subodh	5/9/19 10:11:00 AM

Page 12: [2] Deleted	Acharya,Subodh	5/9/19 10:11:00 AM

Page 12: [2] Deleted	Acharya,Subodh	5/9/19 10:11:00 AM

Page 12: [2] Deleted	Acharya,Subodh	5/9/19 10:11:00 AM

Page 12: [2] Deleted	Acharya,Subodh	5/9/19 10:11:00 AM

Page 12: [2] Deleted	Acharya,Subodh	5/9/19 10:11:00 AM

Page 12: [2] Deleted	Acharya,Subodh	5/9/19 10:11:00 AM

Page 12: [2] Deleted	Acharya,Subodh	5/9/19 10:11:00 AM

Page 12: [2] Deleted	Acharya,Subodh	5/9/19 10:11:00 AM

Page 12: [2] Deleted	Acharya,Subodh	5/9/19 10:11:00 AM

Page 12: [2] Deleted	Acharya,Subodh	5/9/19 10:11:00 AM

Page 12: [2] Deleted	Acharya,Subodh	5/9/19 10:11:00 AM

Page 12: [2] Deleted	Acharya,Subodh	5/9/19 10:11:00 AM

Page 12: [3] Deleted	Acharya,Subodh	5/9/19 10:11:00 AM

Page 12: [3] Deleted	Acharya,Subodh	5/9/19 10:11:00 AM